Drastic Reduction of Plasmon Damping in Two-Dimensional Electron Disks

P. A. Gusikhin, V. M. Muravev, A. A. Zagitova, and I. V. Kukushkin
Institute of Solid State Physics, RAS, Chernogolovka 142432, Russia

(Received 1 June 2018; published 25 October 2018)

In this Letter, plasmon damping has been investigated using resonant microwave absorption of two-dimensional electrons in disks with different diameters. We have found an unexpected drastic reduction of the plasmon damping in the regime of strong retardation. This finding implies large delocalization of the retarded plasmon field outside the plane of the two-dimensional electron system. A universal relationship between the damping of plasmon polariton waves and the retardation parameter is reported.

DOI: 10.1103/PhysRevLett.121.176804

Studies of plasma excitations in two-dimensional electron systems (2DESs) have attracted an increasing interest in recent years [1,2]. This interest has been triggered by the discovery of a new part of the 2D plasmon spectrum, where coupling with light is especially strong [3,4]. This regime, where the influence of the retardation is important, can be realized when the plasmon and light wavelengths are comparable. The influence of electrodynamic effects can be quantified by the retardation parameter A, defined as the ratio of the frequency of the quasi-static 2D plasmon ω_p and the frequency of light in the medium $\omega_{\text{light}} = cq/\sqrt{\varepsilon}$ with the same wave vector q [5]. Therefore,

$$A = \frac{\omega_p(q)}{\omega_{\text{light}}(q)} = \sqrt{\frac{n_s e^2}{2m^* \varepsilon_0 \bar{\varepsilon}} q}\, \frac{1}{\omega_{\text{light}}(q)} \sim \sqrt{\frac{n_s}{q}}, \qquad (1)$$

where n_s and m^* are the density and effective mass of the 2D electrons, respectively. Here, the effective permittivity of the surrounding medium $\bar{\varepsilon} = (\varepsilon + 1)/2$ is the average between the dielectric constants of GaAs ($\varepsilon = 12.8$) and free space. These experiments revealed very interesting and fully unexpected features of the 2D magnetoplasmon spectra. It has been shown that in the small wave-vector and high-density regimes, where the influence of the retardation effects is prominent, there is a strong reduction of the resonant plasma frequency along with very unusual zigzag behavior in the presence of a B field.

These experiments served as a benchmark for a plethora of research in the field of 2D plasma electrodynamics, such as the strong and ultrastrong coupling between 2D electrons and photonic cavity mode [6–10], superradiant Dicke decay of the 2D electron ensemble [11–13], and fine structure of the cyclotron resonance [13]. It is widely accepted that retardation is associated with a dramatic broadening of the plasmon polariton resonance [14–18]. The main reason for this is a significant increase of radiative decay. This has limited the progress of research in the direction of plasmonic systems placed in the regime of ultrastrong retardation—the regime which is potentially very attractive for plasmonic applications [19–21].

In this Letter, we systematically studied the plasmon damping in 2DES disks as a function of their diameter. The measurements reveal that, in contrast to general belief, there is a drastic suppression of plasmon damping in the regime of strong retardation. Our results allowed us to draw important conclusions about the delocalization of retarded plasmon field outside the plane of 2DES. Moreover, we established a universal relation between the damping of plasmon polariton waves and the retardation parameter. These results pave the way for research in the field of ultrastrong light-matter interaction.

This study was performed using a set of high-quality $GaAs/Al_xGa_{1-x}As$ ($x = 0.3$) heterostructures hosting a 2DES in a (20–30) nm quantum well. The electron density was in the range of 0.8 to 6.0×10^{11} cm^{-2}, with an electron transport mobility in the range of 0.5 to 12×10^6 cm^2/(V s). Disk-shaped mesas with diameters in the range of 0.05 to 12 mm were fabricated from these heterostructures. The plasma wave in the disk was excited by electromagnetic radiation guided to the sample either through the waveguide section or with a coaxial cable. The detailed description of the experimental scheme is given in the Supplemental Material I [22]. In the latter case, the radiation from the coaxial cable was transferred to the 2DES through a coplanar waveguide transmission line. In order to detect 2D electron plasma excitations, we employed a noninvasive optical technique of microwave absorption detection [25,26]. This technique relies on the high sensitivity of the 2DES luminescence spectra to 2D-electron heating caused by the absorption of incident microwave radiation. In this technique, 2DES luminescence spectra with and without microwave radiation were collected using a spectrometer with a liquid-nitrogen cooled charge-coupled device camera. The resulting differential spectrum reveals microwave-caused 2DES temperature heating. Therefore, the integral of the absolute value of the differential spectrum could be used as a measure of the

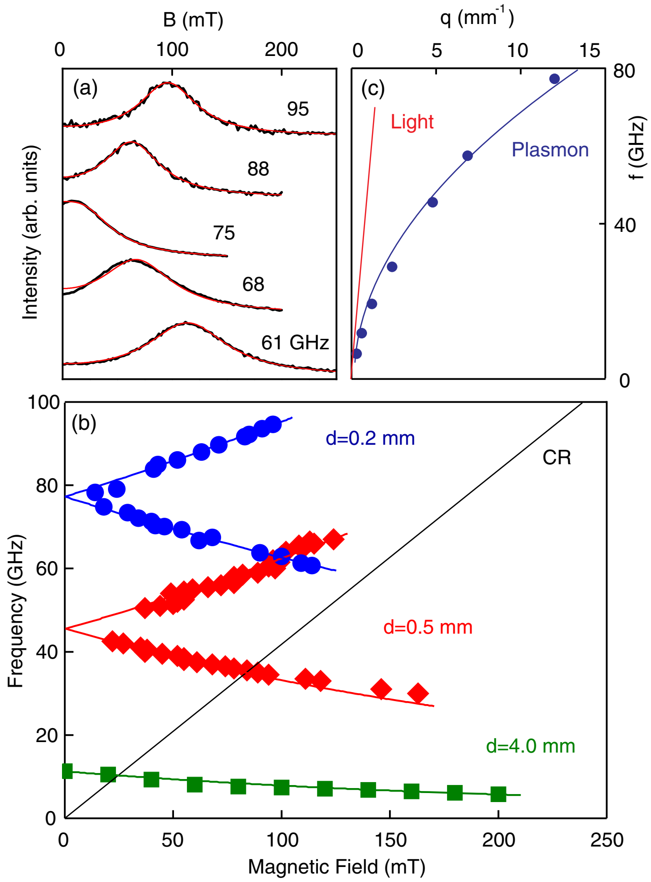

FIG. 1. (a) Evolution of the microwave absorption resonances with the excitation frequency for the 2DES disk with a diameter of $d = 0.2$ mm and electron density of $n_s = 6 \times 10^{11}$ cm^{-2}, the frequency is in the range of 60 to 100 GHz. The curves are offset vertically for clarity. (b) Magnetic-field dependences of the plasmon polariton frequency for the 2DES disks with different diameters. (c) Dispersion of the hybrid plasmon polariton excitation. The solid lines represent the theoretical prediction of 2D plasmon polariton spectrum and dispersion of the light $\omega_{\text{light}} = cq$.

microwave absorption by the 2DES. In our experiments, we used a 780 nm stabilized semiconductor laser with a net output power of 4 mW to excite 2D luminescence, and single-grating spectrometer with a spectral resolution of 0.25 meV to analyze the luminescence spectra. All of the experiments were performed in the liquid helium with a superconducting magnet at a base temperature of $T = 4.2$ K. The magnetic field was directed perpendicular to the sample surface and swept in the range of (0–0.5) T.

Figure 1(a) shows the experimental magnetic-field dependences of the microwave absorption at different frequencies in a 2DES disk with a diameter of $d = 0.2$ mm and electron density of $n_s = 6 \times 10^{11}$ cm^{-2}. For convenience, the curves are shifted vertically. Each of the curves shows resonance occurring at different magnetic-field values. The resonance corresponds to the excitation of the plasma oscillation in the disk. In order to obtain the resonance position and half-width, each magnetoabsorption curve was fitted using a theory that considers both resonant heating and nonresonant Drude absorption [solid lines in Fig. 1(a)]. The detailed fitting procedure is described in the Supplemental Material, part II [22]. Figure 1(b) shows the magnetic-field values at which plasmon resonances occur as a function of the microwave frequency f for the disks with diameters of 0.2, 0.5, and 4.0 mm. The theoretical prediction for the magnetodispersion of plasma waves in the 2DES disks is [27,28]

$$\omega = \sqrt{\omega_p^2 + \left(\frac{\omega_c}{2}\right)^2} \pm \frac{\omega_c}{2}, \tag{2}$$

where $\omega_c = eB/m^*$ is the cyclotron frequency. In the presence of the retardation effects this dependency is modified [3,4,15]. Both the zero-field plasmon frequency and the slope of the magnetodispersion dependency decrease. By fitting the theoretical prediction to the data [solid curves in Fig. 1(b)], we can obtain the zero-field plasmon frequency. For the disk under consideration ($d = 0.2$ mm), the zero magnetic field plasmon frequency $f_p(0) = 78$ GHz. We assign to each plasmon mode a wave vector $q = 2.4/d$ [3]. The experiments of Fig. 1(a) were performed for a series of 2DES disks with diameters of $d = 0.05$, 0.1, 0.2, 0.35, 0.5, 1, 2, 4, and 8 mm. The resultant long-wavelength part of the plasmon polariton dispersion at $B = 0$ T is plotted in Fig. 1(c). The solid curve represents the theoretical 2D plasmon polariton dispersion [3]. The dispersion of light is also shown in the same figure. The plasmon polariton dispersion strongly deviates from the quasistatic $\sqrt{q}$ law, and asymptotically tends to the light line $\omega = cq$ in the limit of a large retardation.

The red circles in Fig. 2(a) represent the dependence of the normalized plasmon polariton half-width $\Delta\omega\tau$ on the retardation parameter A. The retardation parameter is calculated using the definition of Eq. (1). The resonance half-width was determined by two mutually consistent methods. The first method directly utilizes frequency scans at $B = 0$ T (see inset in Fig. 3). The second method uses magnetic-field scans at a fixed microwave frequency. The polariton half-width $\Delta\omega$ is then obtained from the half-width of the polariton resonance in B sweeps multiplied by the magnetodispersion slope $\Delta\omega = (\partial\omega/\partial B)\Delta B$. The ΔB was obtained by fitting the experimental absorption curves using the theory that considers both resonant heating and nonresonant Drude absorption (see Supplemental Material, part II [22]). We verified that both methods yield the same value of $\Delta\omega$ for a series of studied disks.

Figure 2(a) also shows the normalized plasmon frequency ω/ω_p as a function of A (blue squares). It is remarkable that the plasmon half-width $\Delta\omega\tau$ drastically decreases with A. Moreover, the $\Delta\omega\tau$ decreases significantly faster than the resonance frequency ω/ω_p. These

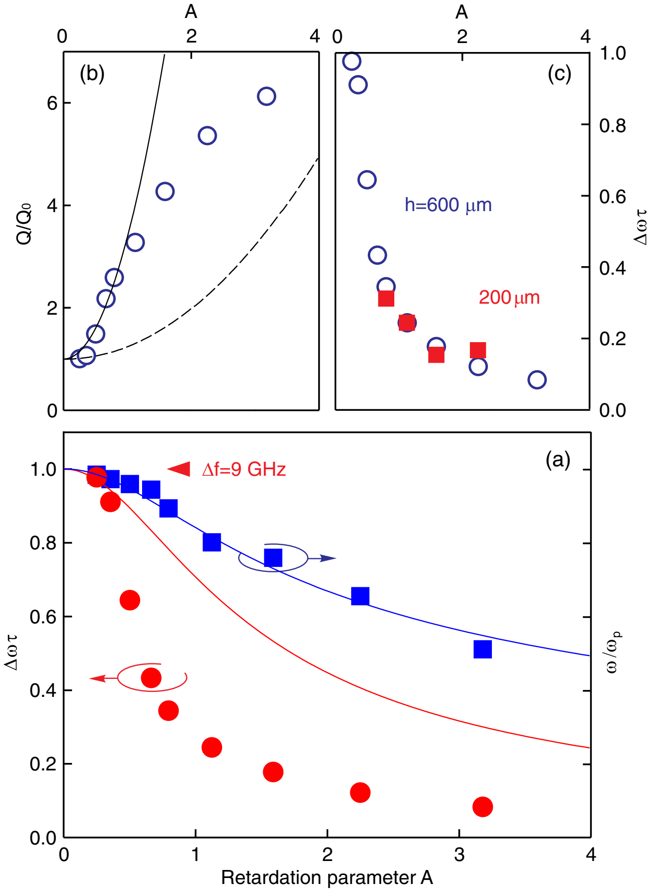

FIG. 2. (a) Normalized plasmon damping $\Delta\omega\tau$ (red circles) and frequency ω_p/ω_0 (blue squares) as a function of the retardation parameter A. The solid lines represent the theoretical prediction based on Eq. (5). (b) Dependence of the normalized Q factor, Q/Q_0, of the plasmon polariton excitation on the retardation parameter A. The curves represent the quadratic fitting to the experimental points (solid) and theoretical prediction based on Eq. (6) (dashed). (c) Comparison of the normalized plasmon half-widths $\Delta\omega\tau$ measured for the samples with thicknesses of $h = 0.6$ mm (open circles) and $h = 0.2$ mm (filled squares).

results imply that the retarded plasmon field is concentrated in a region λ_z, significantly larger than the $\lambda = 2\pi/q$ region in which the dissipation occurs [23]. Indeed, the plasmon polariton damping can be estimated by the formula (we present a precise theoretical derivation in the Supplemental Material, part III [22]):

$$\Delta\omega = \frac{1}{\tau} \times \frac{\lambda}{\lambda_z}. \tag{3}$$

The delocalization of the plasmon mode perpendicular to the 2DES plane is determined by $q_z = \sqrt{q^2 - \omega^2/c^2}$. This relation is a direct consequence of the Maxwell's equations for the bound electromagnetic wave propagating along the 2DES, $\Delta\vec{E} = (\omega^2/c^2)\vec{E}$. Considering the retardation effects, the plasmon polariton dispersion can be very simply expressed as [5]:

$$q^2 = \frac{\omega^2}{c^2} + \left(\frac{\omega^2}{n_s e^2/2m^*\varepsilon_0}\right)^2. \tag{4}$$

By combining Eqs. (3) and (4), we can derive the following expressions for the plasmon polariton frequency and damping:

$$\omega^2 = \frac{\omega_p^2}{\sqrt{1+A^2}}, \qquad \Delta\omega = \frac{1}{\tau}\frac{1}{\sqrt{1+A^2}}. \tag{5}$$

In the limit of a not-large retardation, these equations can be expanded in series, leading to

$$Q = \frac{\omega}{\Delta\omega} = \omega_p\tau(1+A^2)^{1/4} \approx Q_0(1 + A^2/4). \tag{6}$$

We denoted the nonretarded plasmon resonance Q factor as $Q_0 = \omega_p\tau$. It should be noted that Eq. (3) is similar to suppression of the atomic spontaneous emission occurring in the resonator with a unitary Q factor. This effect has been originally predicted by Purcell [29]. The coincidence is not accidental, it stems from the unified nature of all electrodynamic phenomena.

Formula (5) predicts that $\Delta\omega\tau$ decreases with A faster than the frequency ω/ω_p. This is consistent with our experimental results in Fig. 2(a). However, although the plasmon polariton frequency closely follows the theory [blue line in Fig. 2(a)], the resonance narrows with the increase of the retardation parameter significantly faster than the theoretical prediction [red line in Fig. 2(a)]. In order to establish a direct comparison with our theory, we plot the normalized Q factor, Q/Q_0, as a function of the retardation parameter A [Fig. 2(b)]. The solid line in Fig. 2(b) represents a quadratic function $1 + kA^2$ ($k = 2.4$) fitting. The experimental data closely follow the quadratic dependence for a relatively small retardation ($A < 1$). This quantitatively agrees with Eq. (6), albeit the plasmon damping is suppressed relative to the theory [dashed line in Fig. 2(b)]. One may assume that suppression of the plasmon polariton damping is associated with an effect of the semiconductor substrate. In order to test this possibility, we performed measurements (Fig. 2) on the same set of samples thinned from the original $h = 0.6$ mm to $h = 0.2$ mm. Figure 2(c) shows a comparison of the normalized plasmon half-widths $\Delta\omega\tau$ measured for the samples with thicknesses of $h = 0.6$ mm (open circles) and $h = 0.2$ mm (filled squares). The main observation to note is that the substrate thickness does not affect the plasmon polariton damping. We can speculate that a more adequate theoretical consideration for the retardation in the studied 2DES geometry is certainly imperative. The discovered phenomenon is significant in terms of both physics and technology.

One of the most important predictions of the theory is that there is a universal relationship between the normalized

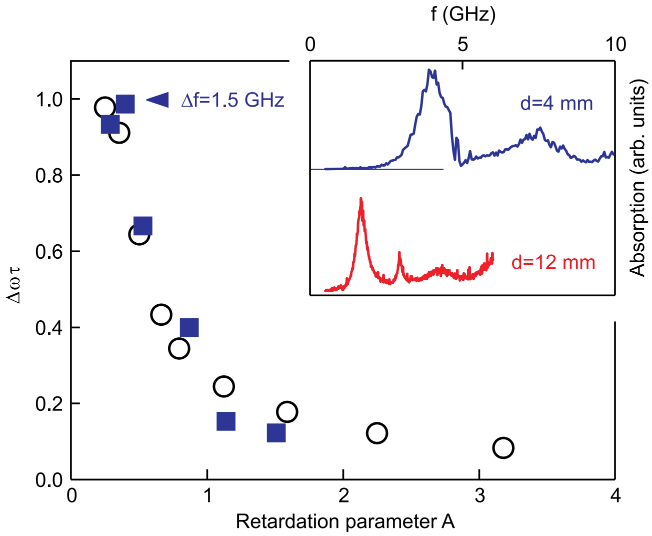

FIG. 3. Normalized resonance half-width at $B = 0$ T as a function of the retardation parameter A. The empty circles correspond to the measurements performed on a wafer with $n_s = 6 \times 10^{11}$ cm^{-2} and $1/\tau = 5.6 \times 10^{10}$ s^{-1}. The blue squares represent the samples fabricated from different wafers with $n_s = 0.8 \times 10^{11}$ cm^{-2} and $1/\tau = 9.5 \times 10^{9}$ s^{-1}. Both dependences are identical. The inset shows microwave absorption spectra measured directly by the frequency scans at $B = 0$ T for the 2DES disks with diameters of $d = 4$ and 12 mm.

plasmon damping $\Delta\omega\tau$ and retardation parameter A. In order to investigate this relation, we repeated the experiment of Fig. 2 for 2DES disks fabricated from three different wafers in terms of density n_s and relaxation time τ. Figure 3 shows the normalized plasmon polariton half-width $\Delta\omega\tau$ as a function of the retardation parameter A. The measurements were performed for two wafers with electron densities and relaxations of $n_s = 6 \times 10^{11}$ cm^{-2} and $1/\tau = 5.6 \times 10^{10}$ s^{-1} (empty circles), and $n_s = 0.8 \times 10^{11}$ cm^{-2} and $1/\tau = 9.5 \times 10^{9}$ s^{-1} (blue squares), respectively. The plasmon normalized dampings for the samples fabricated from the two wafers indeed have an identical dependence on the parameter A. The same universal dependence was also reproduced for the third wafer with $n = 3.9 \times 10^{11}$ cm^{-2} and $1/\tau = 3.4 \times 10^{10}$ s^{-1} (see Supplemental Material, part IV [22]). The discovered universality has a remarkably general nature and is applicable to any type of 2D plasmons.

In conclusion, we have investigated resonant microwave absorption in 2DES disks with diameters in the range of $d = 0.05$ to 12 mm. The plasmon polariton mode excited in the disks has been detected by the optical technique. We have demonstrated an unexpected anomalous suppression of the plasmon damping when the retardation became important. Remarkably, the dependence of the normalized resonance half-width $\Delta\omega\tau$ on the retardation parameter A has a universal character and does not depend on the 2DES parameters and semiconductor substrate thickness.

We thank L. S. Levitov and V. A. Volkov for the stimulating discussions. The authors gratefully acknowledge the financial support from the Russian Science Foundation (Grant No. 14-12-00693).

[1] D. Heitmann, Surf. Sci. **170**, 332 (1986).
[2] J. Łusakowski, Semicond. Sci. Technol. **32**, 013004 (2017).
[3] I. V. Kukushkin, J. H. Smet, S. A. Mikhailov, D. V. Kulakovskii, K. von Klitzing, and W. Wegscheider, Phys. Rev. Lett. **90**, 156801 (2003).
[4] I. V. Kukushkin, V. M. Muravev, J. H. Smet, M. Hauser, W. Dietsche, and K. von Klitzing, Phys. Rev. B **73**, 113310 (2006).
[5] F. Stern, Phys. Rev. Lett. **18**, 546 (1967).
[6] G. Günter, A. A. Anappara, J. Hees, A. Sell, G. Biasiol, L. Sorba, S. De Liberato, C. Ciuti, A. Tredicucci, A. Leitenstorfer, and R. Huber, Nature (London) **458**, 178 (2009).
[7] Y. Todorov, A. M. Andrews, R. Colombelli, S. De Liberato, C. Ciuti, P. Klang, G. Strasser, and C. Sirtori, Phys. Rev. Lett. **105**, 196402 (2010).
[8] V. M. Muravev, I. V. Andreev, I. V. Kukushkin, S. Schmult, and W. Dietsche, Phys. Rev. B **83**, 075309 (2011).
[9] G. Scalari, C. Maissen, D. Turcinkova, D. Hagenmüller, S. De Liberato, C. Ciuti, C. Reichl, D. Schuh, W. Wegscheider, M. Beck, and J. Faist, Science **335**, 1323 (2012).
[10] Q. Zhang, M. Lou, X. Li, J. L. Reno, W. Pan, J. D. Watson, M. J. Manfra, and J. Kono, Nat. Phys. **12**, 1005 (2016).
[11] Q. Zhang, T. Arikawa, E. Kato, J. L. Reno, W. Pan, J. D. Watson, M. J. Manfra, M. A. Zudov, M. Tokman, M. Erukhimova, A. Belyanin, and J. Kono, Phys. Rev. Lett. **113**, 047601 (2014).
[12] T. Laurent, Y. Todorov, A. Vasanelli, A. Delteil, C. Sirtori, I. Sagnes, and G. Beaudoin, Phys. Rev. Lett. **115**, 187402 (2015).
[13] V. M. Muravev, I. V. Andreev, S. I. Gubarev, V. N. Belyanin, and I. V. Kukushkin, Phys. Rev. B **93**, 041110(R) (2016).
[14] C. Sönnichsen, T. Franzl, T. Wilk, G. von Plessen, J. Feldmann, O. Wilson, and P. Mulvaney, Phys. Rev. Lett. **88**, 077402 (2002).
[15] S. A. Mikhailov and N. A. Savostianova, Phys. Rev. B **71**, 035320 (2005).
[16] H. Baida, P. Billaud, S. Marhaba, D. Christofilos, E. Cottancin, A. Crut, J. Lerme, P. Maioli, M. Pellarin, M. Broyer, N. Del Fatti, F. Vallee, A. Sanchez-Iglesias, I. Pastoriza-Santos, and L. M. Liz-Marzan, Nano Lett. **9**, 3463 (2009).
[17] M. Bosman, E. Ye, S. F. Tan, C. A. Nijhuis, J. K. W. Yang, R. Marty, A. Mlayah, A. Arbouet, C. Girard, and M.-Y. Han, Sci. Rep. **3**, 1312 (2013).
[18] I. V. Andreev, V. M. Muravev, V. N. Belyanin, and I. V. Kukushkin, Appl. Phys. Lett. **105**, 202106 (2014).
[19] E. A. Shaner, M. Lee, M. C. Wanke, A. D. Grine, J. L. Reno, and S. J. Allen, Appl. Phys. Lett. **87**, 193507 (2005).
[20] W. Knap, M. Dyakonov, D. Coquillat, F. Teppe, N. Dyakonova, J. Łusakowski, K. Karpierz, M. Sakowicz,

G. Valusis, D. Seliuta, I. Kasalynas, A. Fatimy, Y. M. Meziani, and T. Otsuji, J. Infrared, Millimeter, Terahertz Waves **30**, 1319 (2009).

[21] V. V. Popov, D. V. Fateev, T. Otsuji, Y. M. Meziani, D. Coquillat, and W. Knap, Appl. Phys. Lett. **99**, 243504 (2011).

[22] See Supplemental Material at http://link.aps.org/supplemental/10.1103/PhysRevLett.121.176804, which includes Refs. [23,24], for detailed information about the experimental scheme, analysis of the plasmon resonance line shape, theory of plasmon polariton spectrum and damping, and additional data on damping of plasmon polariton waves for the third wafer.

[23] V. I. Falko and D. E. Khmelnitskii, Zh. Eksp. Teor. Fiz. **95**, 1988 (1989) [Sov. Phys. JETP **68**, 1150 (1989)].

[24] G. Dresselhaus, A. F. Kip, and C. Kittel, Phys. Rev. **98**, 368 (1955).

[25] B. M. Ashkinadze, E. Linder, E. Cohen, and A. Ron, Phys. Status Solidi **164**, 523 (1997).

[26] I. V. Kukushkin, J. H. Smet, K. von Klitzing, and W. Wegscheider, Nature (London) **415**, 409 (2002).

[27] S. J. Allen, Jr., H. L. Störmer, and J. C. M. Hwang, Phys. Rev. B **28**, 4875 (1983).

[28] S. S. Nazin and V. B. Shikin, Fiz. Nizk. Temp. **15**, 227 (1989) [Sov. J. Low Temp. Phys. **15**, 127 (1989)].

[29] E. M. Purcell, Phys. Rev. **69**, 37 (1946).